Proceedings of The Canadian Society for Mechanical Engineering International Congress 2012
CSME International Congress 2012
June 4-6, 2012, Winnipeg, Manitoba, Canada

ATLAS MECANUM WHEEL JACOBIAN EMPIRICAL VALIDATION

Rahman Ahmad, Peter Toonders, M. John D. Hayes, Robert G. Langlois
Department of Mechanical and Aerospace Engineering
Carleton University
Ottawa, ON., Canada

Abstract— The Atlas motion simulator platform is the focus of a multi-year multi-disciplinary fourth year project at Carleton University. It is a state of the art motion platform that allows for unlimited rotation of a cockpit housed in a 9.5 foot diameter sphere about any axis driven by three mecanum wheels, in addition to three decoupled orthogonal translations provided by a translational motion stage. The inverse of the Jacobian matrix is used to map the required speed of the three mecanum wheels to the desired angular velocity of the sphere. The work reported in this paper examines the validity of the Jacobian and the accuracy of the programs that implement it. It is determined, through a number of tests, that the elements in the matrix are valid and that the sphere rotates at its specified angular velocity vector accurately with acceptably low error.

I. Introduction

The Carleton University Simulator Project (CUSP) is one of the fourth year capstone engineering design projects at Carleton University. It is a multi-year project that features a multi-disciplinary team, having students from Mechanical, Aerospace, and Systems and Computer Engineering departments throughout the project life. Over the last ten years, CUSP has focused on the development of a novel motion simulator platform called Atlas [1]. The Atlas motion platform was introduced as a practical alternative to the Gough-Stewart hexapod architecture [2, 3].

Conventional motion simulator platforms use a Gough-Stewart platform in order to provide the six degrees-of-freedom (DOF) necessary for simulate motion cues. Motions are achieved by varying the lengths of the six active prismatic legs. The issue with this method is that the platform has a relatively small workspace due to the kinematic coupling of the actuators, and the potential for leg interference. There are few simulators in the world that are able to overcome this restriction. One is the Eclipse II motion platform [4], being developed at Seoul National University in Korea. It uses three tethers attached to a circular guide that provide three angular DOF to the central motion platform. Circular guides allow the central platform to continuously rotate about two axes. The major drawback to this architecture is that there is no closed form algebraic model for its kinematics. The velocity level kinematics require estimating parameters numerically. The other arcitecture that is capable of providing unlimited angular displacements is the Desdemona motion platform [5]. The Desdemona simulator, developed by TNO Defence, Security & Safety in The Netherlands, uses a fully gimballed system to allow for rotation about any axis. Its range of motion allows up to 8 meters of horizontal translation, and 2 meters of vertical displacement. However, because of the gimbal arrangement, the orientation workspace is not free of singularities because of the potential of gimbal-lock.

Atlas overcomes the limitations of other motion platforms by providing an unbounded orientation workspace that is singularity free. This is achieved by employing an actuation system that uses three mecanum wheels whose contact points are the vertices of an equilateral triangle. Different linear combinations of mecanum wheel speeds yield angular displacements of the sphere about different axes through its geometric centre. A mecanum wheel, illustrated in the right-hand side of Figure 1, is a wheel that transmits force in the tractional direction while allowing slip transverse to that direction. This is in contrast to the original omni wheel design, also illustrated in Figure 1 on the left, which allows slip in the transverse direction, however two offset races are required [6, 7]. The difficulty with omni-wheels is that the two offset castor roller races inject significant vibrations to the sphere during rotations [8]. The mecanum wheel orientation stage is mounted on a Gough-Stewart platform that is used to provide translational displacements. Although the orienting capability of the Gough-Stewart platform could be used, the decoupling of the orientation and translation workspaces require that it is not.

The Atlas concept emerged from the desire to establish a flexible simulation facility at Carleton University capable of six DOF motion and the ability to accept various cockpit configurations for the purpose of simulating any vehicle type [1]. It was originally believed that by actuating three omni wheels in the correct configuration, it would be possible to rotate the sphere about any axis. It was then necessary to prove the theories on a small scale prototype before further developing the concept into a full-scale motion platform. Hence, in the third year of the project, the Atlas Lite tabletop demonstrator, illustrated in

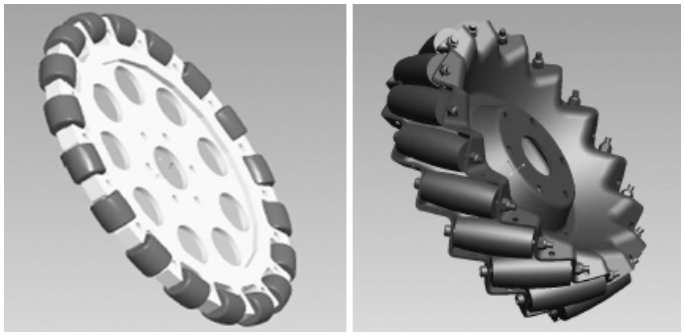

Figure 1. Omni wheel model (left) and mecanum wheel model (right).

Figure 2, was designed and built for testing viability. In the following year surge, sway, and heave stages were added to the platform to generate translations. The resulting motion platform has six DOF with rotation decoupled from translation.

Over the next two years the Atlas Lite platform received additional hardware and software improvements including the development of an inertial orientation sensor (IOS). Work on the Atlas Lite visual orientation system (VOS) was significantly advanced using coloured markers to track absolute sphere orientation. Additionally, a 4 foot diameter half-scale sphere and a sphere support structure were constructed. The purpose of this was to explore composite manufacturing techniques, large-scale actuation of the sphere with omni wheels, as well as to provide further evidence of the feasibility of the design. This model was named the Atlas Technology Demonstrator Platform (TDP).

Year seven brought with it closed-loop control of the Atlas Lite system. The previous in house IOS sensor was replaced with a commercial 3D gyroscope. The VOS system evolved further and a simple sensor fusion algorithm was developed. The TDP sphere was completed and a new base was manufactured, incorporating three drive motors with omni wheels, that was capable of open loop control about the pitch, roll, and yaw directions.

Next, the VOS closed-loop control system of Atlas Lite was implemented with a new marker scheme. Three six inch omni and mecanum wheels were purchased to facilitate dynamic comparison of the wheels on the Atlas TDP. It was discovered it would be unlikely that any omni wheels large enough for the full-scale Atlas prototype would be available. Moreover, it was determined that the vibration due to the shape of the castor rollers in two offset races and the relatively small contact patch between the sphere and castor rollers necessitated the change to mecanum wheels.

Also that year, a new Jacobian was developed to account for the geometry of the mecanum wheels. Material properties for the Atlas TDP composite panels were determined. Research into sandwich composite structures was undertaken for full-scale panel construction and weight reduction. Motor specifications were also chosen for the full-scale Atlas prototype and a new real-time processing system was implemented on Atlas TDP.

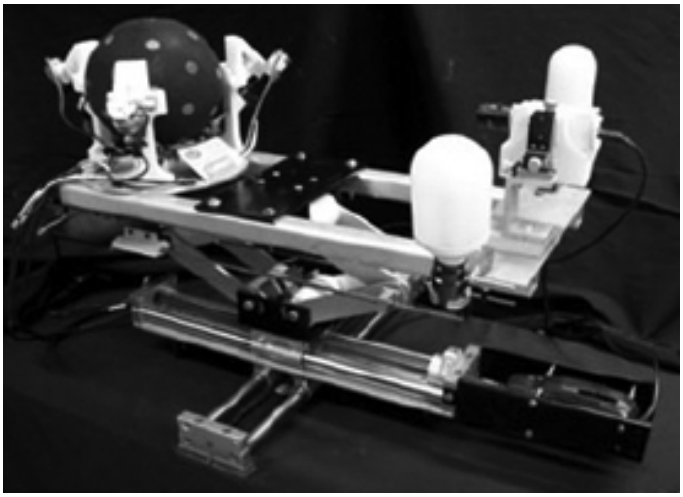

Figure 2. Atlas Lite (2008/2009).

The full-scale prototype is called the *Atlas simulator* and the current 3D solid model is shown in Figure 3. The unique design of Atlas decouples translational actuation in three orthogonal directions from general unbounded rotational actuation about an arbitrary, continuously variable axis. This year has seen the purchase and installation of a MOOG Gough-Stewart platform, the finalized design of many Atlas components, and the manufacturing of support structures and interface platform, illustrated in Figure 3.

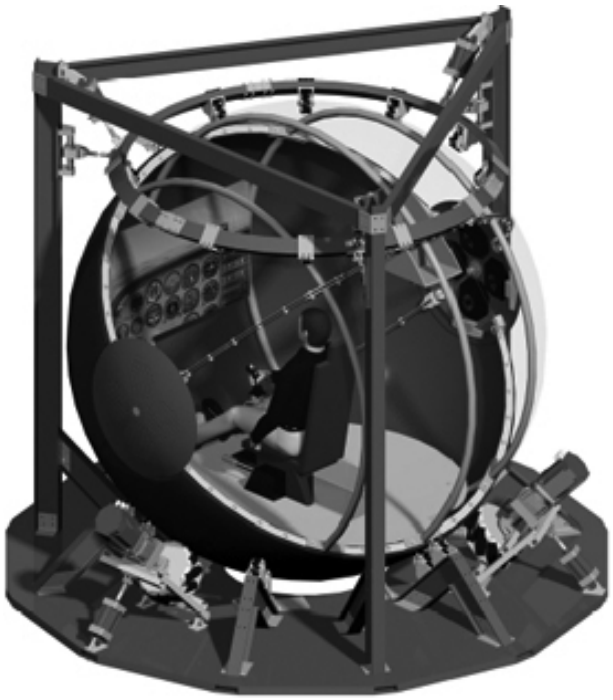

Figure 3. Full-scale Atlas platform concept.

The development of Atlas has been progressing steadily for a decade. As the implementation of the full-scale hardware is completed, elements of the final control system are also being fine-tuned. The main goal of this paper is to investigate the accuracy of the Jacobian matrix and its implementation in driving the active mecanum wheels for Atlas TDP. In order to do this, four different tests were designed and implemented. The analysis of the resulting data has enabled validation of the Jacobian.

II. KINEMATICS

While the use of mecanum wheels for the actuation of Atlas offers a greater range of motion over typical motion simulators, this increased freedom of motion involves more complex kinematics than the standard omni wheel due to castor roller orientation. A Jacobian was developed in [9] to map the angular velocity of the individually driven mecanum wheels to the motion of the Atlas sphere.

A. The Atlas Jacobian

The Atlas Jacobian is a 3×3 matrix that uses the geometry of the mecanum wheel contact point locations and caster roller orientation to populate its nine elements. It has the form [9]:

$$\mathbf{J} = \frac{r}{R} \begin{bmatrix} S\theta_1 & -T\alpha_1 & C\theta_1 \\ S\phi_2 T\alpha + S\theta_2 C\phi_2 & S\phi_2 S\theta_2 - C\phi_2 T\alpha & C\theta_2 \\ S\phi_3 T\alpha + S\theta_3 C\phi_3 & S\phi_3 S\theta_3 - C\phi_3 T\alpha & C\theta_3 \end{bmatrix}^{-1}, \quad (1)$$

whereby

$$\begin{bmatrix} \Omega_x & \Omega_y & \Omega_z \end{bmatrix}^T = \mathbf{J} \begin{bmatrix} \omega_1 & \omega_2 & \omega_3 \end{bmatrix}^T \quad (2)$$

and where S, C, and T are abbreviations for sine, cosine, and tangent, respectively. The nomenclature for Equations (1) and (2) is listed in Table I.

The Jacobian maps the three mecanum wheel angular speeds to the sphere angular velocity. It's nine elements are functions of the geometry of the mecanum wheel contact point locations and caster roller orientation relative to a non-moving coordinate system whose origin is at the geometric centre of the sphere, see Figure 4. The unique property of this Jacobian is that it is time invariant. Each of it's nine elements is a function of fixed geometric design constants which have been selected such that the Jacobian always possesses full rank. This means that the orientation workspace is unbounded and free from configuration and representational singularities.

To generate a desired sphere angular velocity, the Jacobian must be inverted so the three required mecanum wheel speeds can be computed. However, because the Jacobian is free from singularities of any kind, and it's condition number is identically equal to unity, it can always be inverted, yielding the mapping from the angular velocity vector of the sphere to the angular speeds of the three mecanum wheels:

$$\boldsymbol{\omega} = \begin{bmatrix} \omega_1 \\ \omega_2 \\ \omega_3 \end{bmatrix} = \mathbf{J}^{-1} \begin{bmatrix} \Omega_X \\ \Omega_Y \\ \Omega_Z \end{bmatrix}, \quad (3)$$

where,

$$\mathbf{J}^{-1} = \frac{R}{r} \begin{bmatrix} S\theta & -T\alpha_1 & C\theta \\ S\phi_2 T\alpha + S\theta C\phi_2 & S\phi_2 S\theta - C\phi_2 T\alpha & C\theta \\ S\phi_3 T\alpha + S\theta C\phi_3 & S\phi_3 S\theta - C\phi_3 T\alpha & C\theta \end{bmatrix}. \quad (4)$$

B. Jacobian Matrix Constants

The geometry of Atlas' mecanum wheel contact point locations and rollers are illustrated in Figures 4 and 5. The associated angles θ, the angle from the x-y plane of the non-moving coordinate system affixed to the centre of the sphere to the mecanum wheel contact points, which is assumed to be the same for all three wheels; the angles about the non-moving z-axis to each respective mecanum wheel with mecanum wheel 1 being the datum, are $\phi_1 = 0°$, $\phi_2 = 120°$, and $\phi_3 = 240°$; and finally α is the axis angle of the caster roller with respect to the mecanum wheel axis. The variables and constants for Equation (4) are summarized in Table I.

III. EXPERIMENTAL TEST PLAN

To drive the wheels, a LabVIEW VI uses the inverse Jacobian to achieve the desired sphere angular velocity. Therefore, validating the inverse Jacobian is an important step in the development of the Atlas TDP, and the full-scale Atlas prototype. A series of tests was created in order to systematically check the validity of the Jacobian. For all tests performed, it was chosen that 42 different angular velocities would be used to obtain results. All sampled data within the same angular velocity profile was averaged to ensure consistent results. The tests performed were on the half-scale Atlas TDP, and the results are expected to reflect the full scale model. Furthermore, the tests were performed using open-loop control, whereas the full-scale model is expected to run closed-loop control, and thereby enhance accuracy by controlling error.

Test 1 was designed to verify that the inverse Jacobian is properly calculated by LabVIEW and that its output is equal to the output read by the virtual encoders on the Atlas TDP. This verifies that the specified input is what the encoders are reading. During these tests, a sample population of 60, or greater, was used and averaged to compare to the expected results during each of the 42 trials. Agreement between the computed inverse Jacobian and motor encoders implies that the inverse Jacobian is being computed properly within LabVIEW, and the motors are receiving the proper command input from the software to achieve the prescribed angular velocity of the sphere.

Test 2 involves using a timer to establish how long it takes for the mecanum wheels to complete N rotations, where N is the number of rotations such that the elapsed time of the

TABLE I. Jacobian variables and constants for the Atlas TDP.

SYMBOL	DESCRIPTION	TYPE	VALUE
Ω_x	Sphere angular velocity about the x-axis (roll)	Input	-
Ω_y	Sphere angular velocity about the y-axis (pitch)	Input	-
Ω_z	Sphere angular velocity about the z-axis (yaw)	Input	-
R	Radius of sphere	Constant	24.127 in
r	Radius of mecanum wheel	Constant	3.005 in
θ	Angle from sphere center to the center of the active mecanum wheels	Constant	51.4 °
ϕ_1	Angle about the z-axis to mecanum wheel 1	Constant	0°
ϕ_2	Angle about the z-axis to mecanum wheel 2	Constant	240°
ϕ_3	Angle about the z-axis to mecanum wheel 3	Constant	120°
α	Angle between the mecanum roller and the contact patch of the sphere	Constant	45°
ω_1	Mecanum wheel 1 angular speed	Output	-
ω_2	Mecanum wheel 2 angular speed	Output	-
ω_3	Mecanum wheel 3 angular speed	Output	-

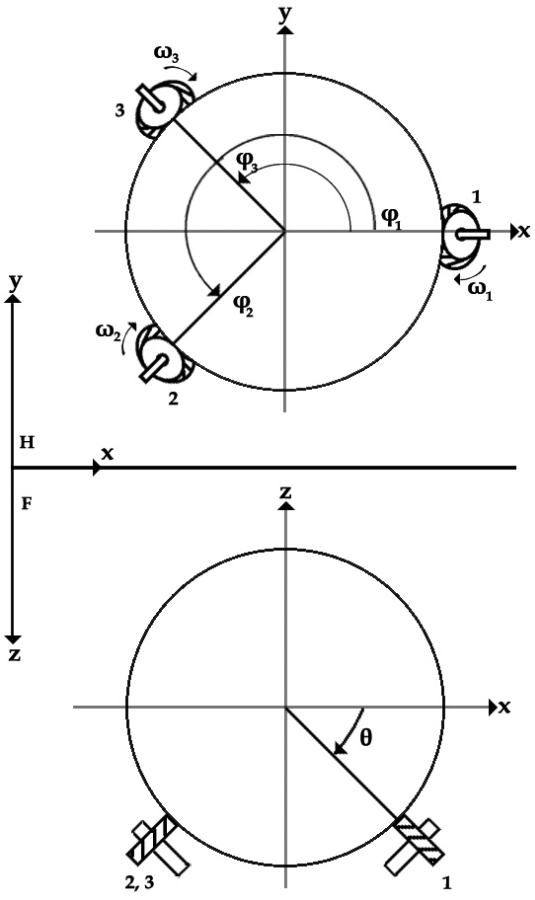

Figure 4. Configuration of three driven wheels for Atlas.

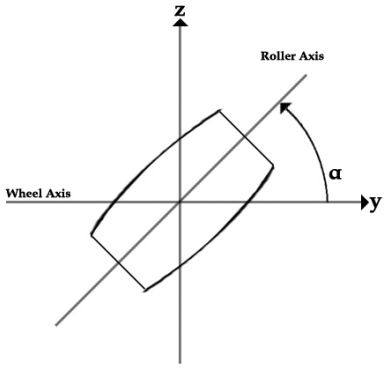

Figure 5. Mecanum wheel roller axis for Atlas.

test is greater than 30 seconds. Then the motor angular speed calculated by the time interval and number of rotations is compared to the angular speed recorded by the virtual encoders and to the computed Jacobian, to verify that the motors are spinning at the correct rate as indicated by the software. This is done for all 42 angular velocities. The accuracy of the tests is estimated to be $1/16^{\text{th}}$ of a period of a wheel rotation. The first and second tests of the validation process do not explicitly validate the inverse Jacobian, but rather ensure the model is performing as expected in order to carry out the Jacobian validation.

Test 3 establishes the axis about which the sphere rotates given a prescribed angular velocity. From the sphere's motion, the angular acceleration is measured using an Xsens MTi 3D Motion Tracker IOS. The benefit of using the Xsens sensor is that it can immediately output angular velocity, and thereby eliminates the need to integrate within LabVIEW. The IOS is mounted onto a rigid beam in the middle of the sphere, and is calibrated such that all inputs were zeroed. The sphere is run for 42 different angular velocities, data exported to Microsoft Excel, and the average of a minimum of 30 samples for each angular velocity was computed for each of the 42 angular velocities.

Test 4 examined the trueness of the sphere's rotation. The sphere is commanded to rotate for exactly one revolution for all

42 angular velocity inputs based on the time required to perform one revolution. An OptoTrak Certus motion capture system compares initial and final orientation coordinates of markers on the sphere. Based on these coordinates, the chord between the sphere's original and final orientations can be calculated, and the displacement arc of the sphere is able to be calculated based on the radius of the model, and the chord length. The displacement is the absolute error in the system, should any exist. Though Test 3 implicitly validates Test 4, it is still needed for error quantification.

When a problem arose during testing, it was isolated, reviewed, corrected, and all tests repeated. These four above-mentioned tests serve to empirically validate the Atlas Jacobian.

IV. Experimental Results and Errors

The tests were carried out on the Atlas TDP, and after much troubleshooting of both software and hardware, the results reflect the true Atlas model. The empirical results for each of the four tests were plotted, analyzed, and compared to the theoretical expected value based on the Jacobian matrix elements and the angular velocity of the sphere. Plausible errors for each test are discussed in this section. During Test 1, the inverse Jacobian is calculated in LabVIEW and the signal is sent to the motors to spin at the required angular speed to achieve the sphere's angular velocity. The test observed that the Jacobian input was indeed very close to virtual encoder output.

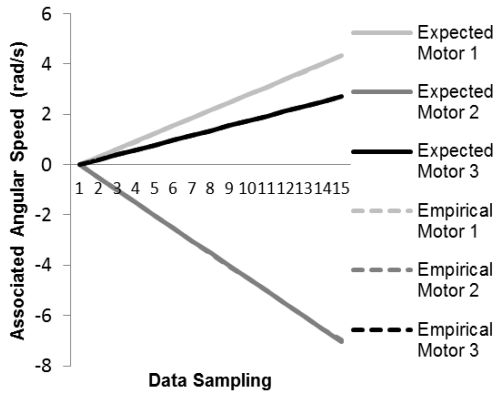

Figure 6. Jacobian vs. virtual encoders (rad/s) about x-axis.

Figure 6 shows the angular speed of each motor compared to the Jacobian input to the system for the sphere's angular velocity about the x-axis. Similarly, Figure 7 shows the result about the y-axis, and Figure 8 about the z-axis. Considering the system is in open-loop control, the Jacobian and encoders agree within reason and are considered satisfactory. Errors for each motor averaged for all tests are listed in Table II, and can be attributed to backlash in the motor gearboxes, as well as fluctuations in the encoder data logged during the tests.

For Test 2, a stopwatch was used to count the time taken for each mecanum wheel to complete N rotations, where number of rotations is such that the time elapsed for the test is a minimum

Table II. Motor errors for Test 1.

Motor 1	Motor 2	Motor 3
0.23%	0.18%	0.08%

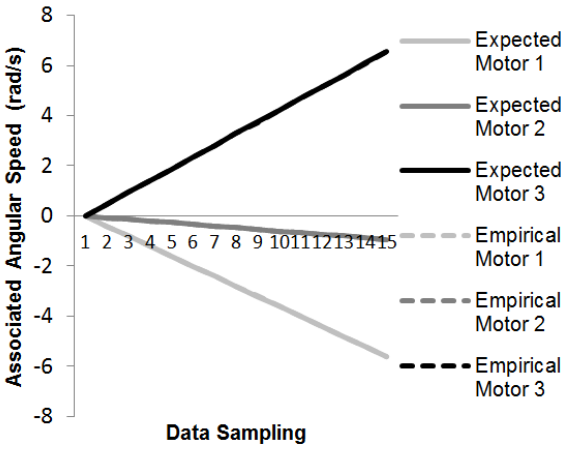

Figure 7. Jacobian vs. virtual encoders (rad/s) about y-axis.

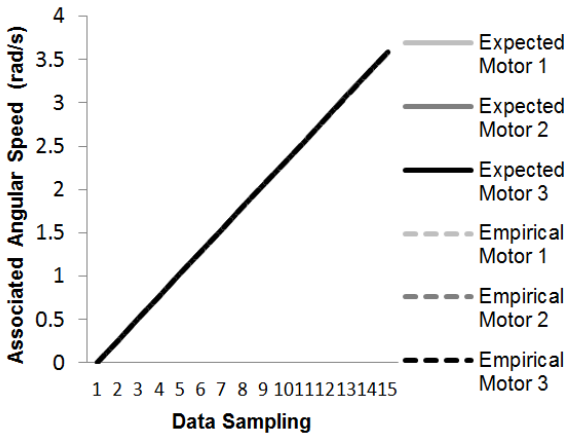

Figure 8. Jacobian vs. virtual encoders (rad/s) about z-axis.

of 30 seconds, and then compared to the expected time elapsed for the 42 angular velocity inputs. The tests observed that the physical motor rotations agreed with the value read by the encoders.

Figure 9 shows the number of rotations required for each motor when the sphere is rotating about the x-axis to achieve 30 seconds of testing. Figure 10 shows the angular speed of each motor being compared to the virtual encoder value for the sphere's angular velocity about the x-axis. Figure 11 shows the number of rotations required for each motor when the sphere is rotating about the y-axis to achieve 30 seconds of testing. Figure 12 shows the motor angular speed for the sphere's angular velocity about the y-axis. Figure 13 shows the number of rotations required for each motor when the sphere is rotating about the z-axis to achieve 30 seconds of testing, whereas

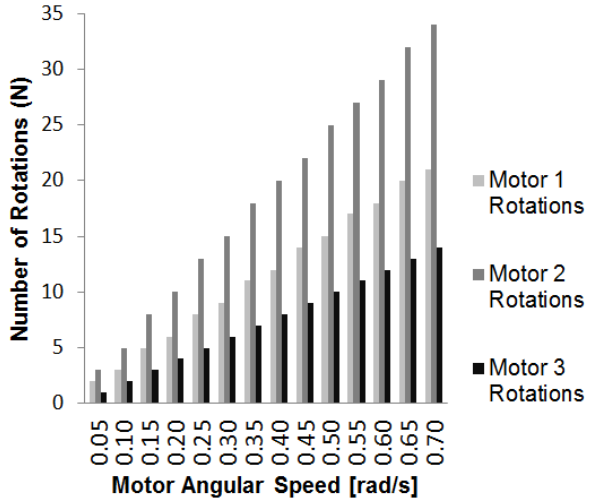

Figure 9. Number of rotations required for each motor about x-axis.

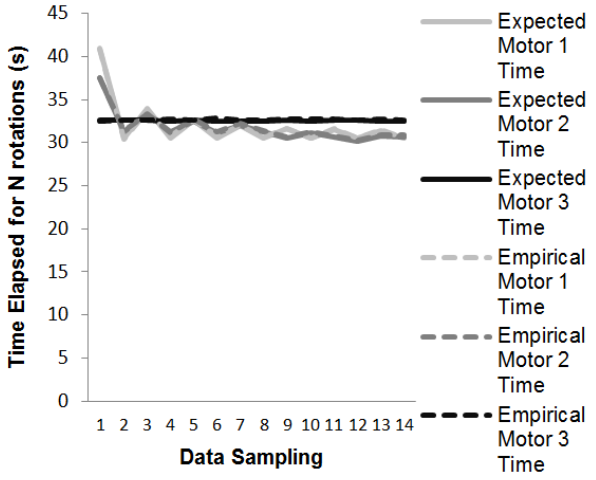

Figure 10. Time taken to for each motor about x-axis.

Figure 14 shows the motor angular speeds for the sphere's angular velocity about the z-axis. The errors listed in Table III can be attributed to the open-loop control and backlash in the system.

TABLE III. Motor errors for Test 2.

Motor 1	Motor 2	Motor 3
0.28%	0.37%	0.36%

Associated errors are higher than those in Test 1 because Test 2 relies on a user to start and stop the timer; however, these errors are deemed to be satisfactory.

Test 3 used an IOS system to measure the angular velocity. The sphere is then run for 42 different angular velocities, and the data exported to Microsoft Excel. The average of a minimum of 30 samples for each angular velocity was taken for each of the 42 angular velocities.

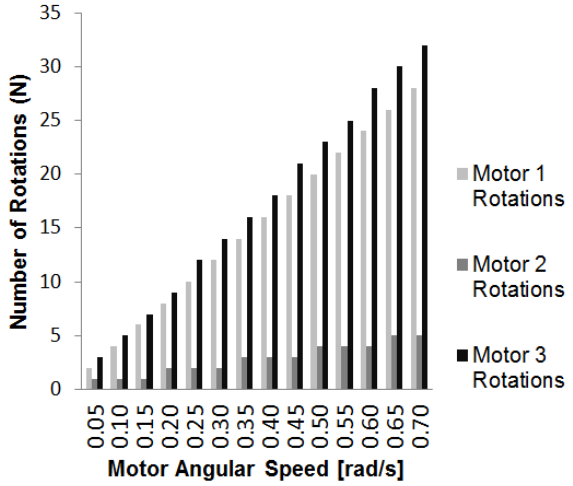

Figure 11. Number of rotations required for motors about y-axis.

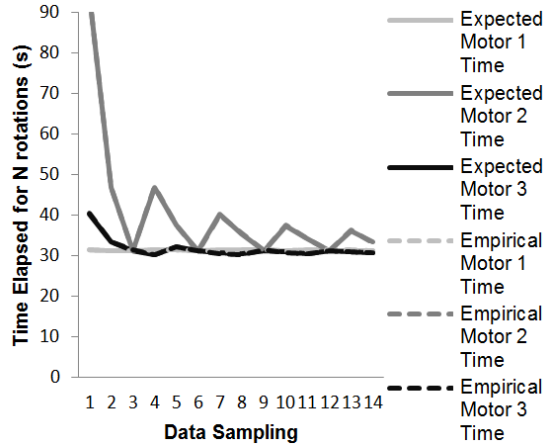

Figure 12. Time taken to for each motor about y-axis.

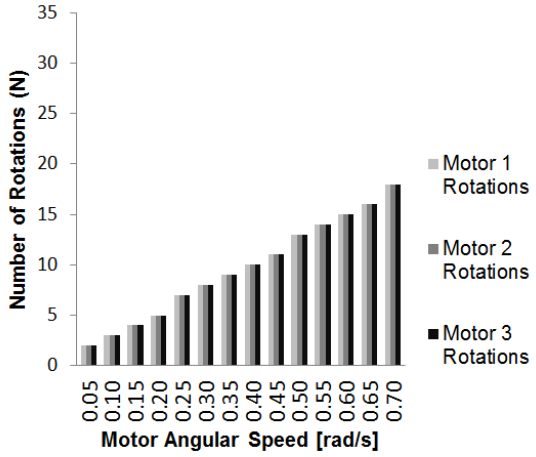

Figure 13. Number of rotations required for each motor about z-axis.

The results indicated that there was considerable error in the sphere's motion. Figures 15, 16, and 17 show how the

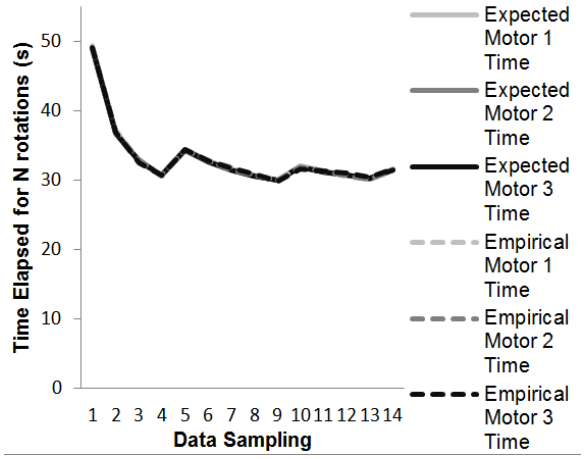

Figure 14. Time taken to for each motor about z-axis.

angular velocities behave about roll, pitch, and yaw axis when commanded to rotate about the x-axis (roll), y-axis (pitch), and z-axis (yaw), respectively.

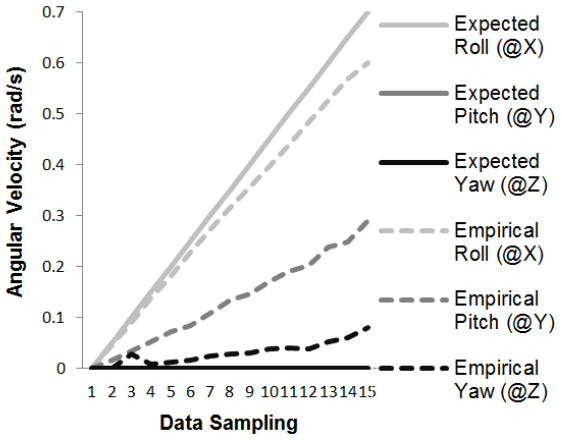

Figure 15. Theoretical vs. experimental angular velocity (rad/s) about x-axis.

Errors computed for roll, pitch, and yaw, listed in Table IV, are much higher than the first two tests. When observing the tests, it is immediately noticeable that high levels of vibration and gyration exist in the sphere's motion, and that these cause the sphere's motion to be jerky. It is also observed that the angular velocity vector direction slowly changes over the course of longer test runs due to this error. This explains the errors increasing as time increases, as shown in the three figures. Because the tests were run continuously, it is unknown if slip is a large factor in the IOS test results; though based on the gyration, it is expected to exist. The sphericity of the model is also questionable, as well as the condition of the sphere, having incurred divots along its surface from general wear and tear.

Test 4 uses the Optotrak Certus to measure the initial and final orientation of the sphere. From the coordinates, the displacement arc between the two points is calculated. The

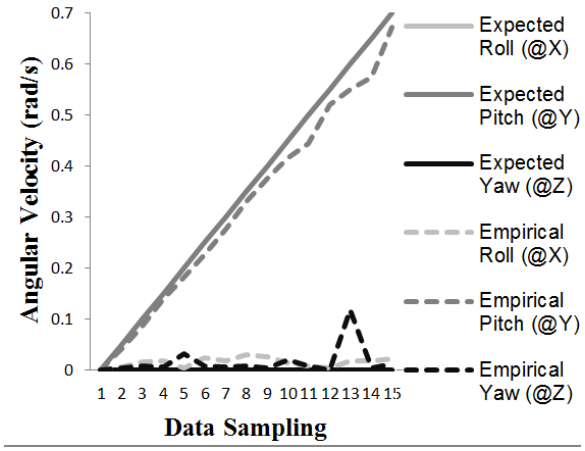

Figure 16. Theoretical vs. experimental angular velocity (rad/s) about y-axis.

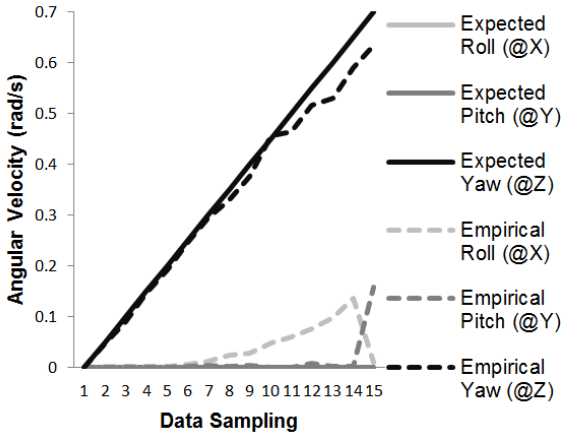

Figure 17. Theoretical vs. experimental angular velocity (rad/s) about z-axis.

results are shown in Figures 18, 19, and 20 for roll, pitch, and yaw, respectively. The errors, shown in Table V, are similar to those during Test 3.

The errors associated with Test 4 are similar to those found in Test 3. Since the tests were run discretely of one another, there is less vibration and gyration present, which accounts for the smaller error. It is evident from this test, however, that slip does exist during starting and stopping, confirming errors associated with Test 3.

V. Conclusion

This paper has presented a model of the angular motion of a composite sphere driven by three mecanum wheels. Four individual tests were used in order to validate the trueness

TABLE IV. Angular velocity vector errors for Test 3.

Ω_x	Ω_y	Ω_z
10.39%	8.61%	5.67%

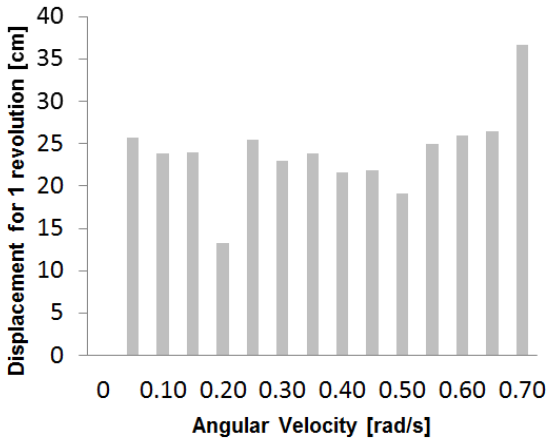

Figure 18. Experimental displacement length for each angular velocity about the x-axis.

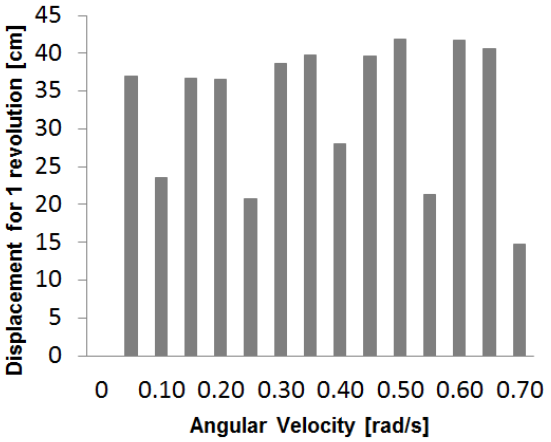

Figure 19. Experimental displacement length for each angular velocity about the y-axis.

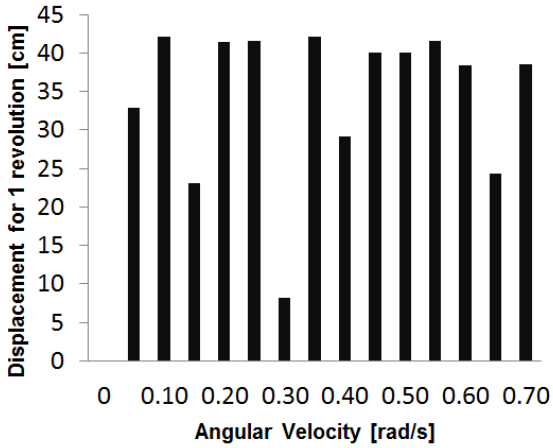

Figure 20. Experimental displacement length for each angular velocity about the z-axis.

TABLE V. Displacement errors for Test 4.

Displacement about X	Displacement about Y	Displacement about Z
6.19%	8.42%	8.83%

of the sphere's rotation. These tests are useful because they can be used to estimate potential sources of error for the full scale Atlas. For instance, the sphericity of the model will be significantly improved for the full-scale model and mechanical error will decrease with the addition of normal loads on the sphere. Secondly, during Tests 3 and 4 it was noted that much of the error could be associated with the gyration and vibration due to imperfect sphere radius. Aside from model and mechanical error, the remainder of the associated error can be attributed to measurement hysteresis.

The full scale Atlas simulator will be one of only a handful of simulators in the world that are capable of a full range of unlimited angular motion. It will allow pilots to gain real flight experience for just about any situation imaginable. The work reported in this paper is just one more step towards the realization of nearly a decade of work and a state of the art motion platform for vehicular simulation.

REFERENCES

[1] M. J. D. Hayes and R. G. Langlois, "Atlas: a Novel Kinematic Architecture for Six DOF Motion Platforms," Transaction of the Canadian Society for Mechanical Engineering, vol. 29 (4), 2005, pp. 701–709.

[2] V. Gough, "Discussion in London: Automobile Stability, Control, and Tyre Performance," Proc. Automobile Division, Institution of Mech. Engrs., 1956, pp. 392–394.

[3] D. Stewart, "A Platform With Six Degrees of Freedom," Proc. Instn. Mech. Engr., vol. 180 (15), 1965, pp. 371–378.

[4] J. Kim, J.-C. Hwang, J.-S. Kim, C. Iurascu, F. C. Park, and Y. M. Cho, "Eclipse-11: a New Parallel Mechanism Enabling Continuous 360-Degree Spinning Plus Three-axis Translational Motions," IEEE Transactions on Robotics and Automation, vol. 18 (3), 2002, pp. 367–373.

[5] W. Bles and E. Groen, "The DESDEMONA Motion Facility: Applications for Space Research," Microgravity Science and Technology, vol. 21 (4), 2009, pp. 281–286.

[6] M. J. D. Hayes, R. G. Langlois, and A. Weiss, "Atlas Motion Platform Generalized Kinematic Model," Meccanica, vol. 46 (1), 2011, pp. 17–25.

[7] A. Weiss, R. G. Langlois, and M. J. D. Hayes, "Unified Treatment of the Kinematic Interface Between a Sphere and Omnidirectional Wheel Actuators," accepted for publication August 9, 2011 in ASME Journal of Mechanisms and Robotics, 2011.

[8] A. Weiss, R. G. Langlois, and M. J. D. Hayes, "The Effects of Dual-Row Omnidirectional Wheels on the Kinematics of the Atlas Spherical Motion Platform," Mechanism and Machine Theory, vol. 44 (2), 2009, pp. 349–358.

[9] J. Plumpton, "Jacobian Derivation," Technical Memorandum, Carleton University, TM-DYN-jp.11.JacobianDerivation.03.pdf, 2011.